



Full length article

The *Penaeus stylirostris* densovirus capsid protein interacts with the *Litopenaeus vannamei* BCCIP protein

Digang Zeng^{a,1}, Min Peng^{a,1}, Qiong Yang^a, Chunling Yang^a, Zhenping Liao^a, Qiangyong Li^b, Qingyun Liu^b, Weilin Zhu^a, Hui Wang^a, Min Li^a, Xiaohan Chen^b, Daxiang Xie^a, Yong Lin^a, Xiuli Chen^{a,**}, Yongzhen Zhao^{b,*}

^a Guangxi Key Laboratory of Aquatic Genetic Breeding and Healthy Aquaculture, Guangxi Academy of Fisheries Sciences, Nanning, China

^b Guangxi Shrimp Breeding Engineering Technology Research Center, Guangxi Academy of Fisheries Sciences, Nanning, China

ARTICLE INFO

Keywords:

Penaeus stylirostris densovirus
Capsid protein
Litopenaeus vannamei
BCCIP

ABSTRACT

Viral capsid proteins play an important role in the viral infection process. To identify the cellular proteins in shrimp that interact with the *Penaeus stylirostris* densovirus capsid protein (PstDENV-CP), we constructed a yeast two-hybrid (Y2H) cDNA library of the muscle tissue of *Litopenaeus vannamei*, and hybridized the bait vector pGBKT7-CP with this library. Cloning and sequencing showed that the shrimp protein interacting with PstDENV-CP was a homolog of BRCA2 and CDKN1A(p21)-interacting protein (BCCIP). We named this protein *L. vannamei* BCCIP (LvBCCIP). Further analysis showed that LvBCCIP interacted with *L. vannamei* calmodulin (LvCaM). We validated the interactions between PstDENV-CP and LvBCCIP, and between LvBCCIP and LvCaM, with GST pull-down assays. The gene expression of *LvBCCIP* increased significantly after PstDENV challenge. In addition, the PstDENV titer of PstDENV-challenged shrimp was significantly reduced after *LvBCCIP* expression was inhibited using double-stranded RNA (dsRNA) interference. These results indicated that LvBCCIP is critical to PstDENV pathogenesis in *L. vannamei*. Interestingly, the growth rate of *L. vannamei* was significantly reduced when *LvBCCIP* gene expression was silenced, indicating that LvBCCIP may also be associated with growth regulation in *L. vannamei*. Thus, the interaction between PstDENV-CP and LvBCCIP might explain why PstDENV infection leads to runt-deformity syndrome in shrimp.

1. Introduction

The Pacific white shrimp (*Litopenaeus vannamei*), also known as the white shrimp or the whiteleg shrimp [1], is one of the three most commonly-farmed shrimp species in the world [2]. However, in recent decades, the *L. vannamei* aquaculture industry has been threatened by several viral pathogens, including white spot syndrome virus, Taura syndrome virus, and *Penaeus stylirostris* densovirus (PstDENV) [3]. PstDENV, also known as infectious subcutaneous and hematopoietic necrosis virus (IHNNV) [4], is particularly important, infecting both farmed and wild shrimp [5]. PstDENV is the smallest of the known shrimp viruses [6]: the PstDMV virion is a non-encapsulated icosahedron with a diameter of 22 nm [6]. The nucleic acid of the PstDMV virion is a 4.1 kb linear single-stranded DNA molecule, containing only three open reading frames (ORFs) [7]. Two of these ORFs encode non-structural proteins (NS1 and NS2), and one ORF encodes the capsid

protein (CP) [7,8]. In *L. vannamei*, PstDENV may lead to runt-deformity syndrome (RDS), which is characterized by slow growth and morphological malformations [9]. Although RDS is generally not fatal [10], this disease causes severe economic losses due to reduced yields and irregular body shapes [11,12]. In order to prevent and effectively treat RDS, a thorough characterization of the molecular mechanism of RDS is urgently needed.

Viral capsids play various necessary roles in viral infections [13]. In non-enveloped viruses, the capsid encapsulates and protects the viral nucleic acid, enabling the initial virus–host interaction [14]. After receptor binding, viruses are internalized by the host cell; the outer viral shell then breaks down, delivering viral genomic and accessory proteins into the host [13]. After the virion invades the host, it interacts with host proteins, blocking normal physiological activities, and causing a series of gene- and protein-regulation disorders [15,16]. Therefore, studying the interaction between the viral capsid and shrimp cellular

* Corresponding author.

** Corresponding author.

E-mail address: 303800733@qq.com (Y. Zhao).

¹ These authors contributed equally to this work.

proteins might clarify the mechanisms by which PstDNV infects shrimp and RDS is triggered.

Here, we aimed to identify the *L. vannamei* cellular proteins that interact with the PstDNV viral capsid using yeast two-hybrid (Y2H) assays; Y2H is powerful technique that detects both transient and stable interactions between proteins [17]. We also aimed to characterize the role of these interactions during the PstDNV infection process and during the growth of infected *L. vannamei* using real-time quantitative PCR (qRT-PCR) and RNA interference.

2. Materials and methods

2.1. Screening for the cellular proteins interacting with PstDNV-CP using Y2H

Total RNA was extracted from the muscle tissue of *L. vannamei* using Trizol reagent (TaKaRa, Japan), following the manufacturer's instructions. Double-stranded cDNA was synthesized using SMART cDNA synthesis kits (TaKaRa, Japan), and short cDNA fragments were removed using CHROMA SPIN TE-400 columns (Clontech, USA). cDNAs were then recombined with pGADT7-Rec vectors (Clontech, USA), and transferred into yeast Y187 (Clontech, USA) to construct a cDNA Y2H library. The primers IN-F and IN-R (Table 1) were designed based on the genomic DNA sequence of PstDNV (GenBank accession no. NC_002190.2) [18] using Primer Premier v6.2 (<http://www.premierbiosoft.com>) [19]. The PstDNV-CP gene sequence was amplified using PCR. The PCR cycling program was as follows: preheating at 94 °C for 30 s; then 35 cycles of 94 °C for 30 s, 58 °C for 30 s and 72 °C for 1 min, and a final extension at 72 °C for 10 min.

The recombinant bait vector pGBKT7-CP was constructed using the Fusion HD Cloning Kit (Clontech, USA), following the manufacturer's instructions. After testing the autoactivation and toxicity of pGBKT7-CP (following the instructions in the Clontech Matchmaker Gold Yeast Two-Hybrid System User Manual), the single colony containing pGBKT7-CP was resuspended in 2 × YPDA medium (Clontech, USA),

mixed with the Y2H library, and transferred to a 2 L conical flask. The flask was incubated at 30 °C with shaking at 45 r/min for 24 h, and then centrifuged at 1000 × g. The precipitate was resuspended in 10 mL of 0.9% NaCl, and 150 μL aliquots of this resuspension were spread on SD/-Ade/-His/-Leu/-Trp plates. Plates were cultured at 30 °C in the dark for 5 days. Clones larger than > 2 mm in diameter were selected and cultured on SD/-Ade/-His/-Leu/-Trp/X-α-Gal/Aba plates at 30 °C in the dark for 5 days. Blue clones were randomly selected and then sequenced by the Beijing Genomics Institute (Beijing, China).

We searched for sequences homologous to the *L. vannamei* gene sequence in GenBank using BLAST (<http://www.ncbi.nlm.nih.gov/BLAST>) [20]. Based on our results, we named the novel gene *LvBCCIP*. The open reading frame (ORF) of *LvBCCIP* was identified with ORF finder (<https://www.ncbi.nlm.nih.gov/orffinder>), while the molecular weight and the isoelectric point of the encoded protein were determined with pI/Mw tool (http://web.expasy.org/compute_pi/). Conserved protein domains were identified with Pfam (<http://pfam.xfam.org/>) [21]. The nine protein sequences most homologous to *LvBCCIP* were downloaded from GenBank. A neighbor-joining (NJ) phylogenetic tree was constructed based on this multiple protein sequence alignment with Mega v5.1 [22].

2.2. Y2H screening for cellular proteins interacting with *LvBCCIP*

To identify cellular proteins interacting with *LvBCCIP*, we designed the primers BC-F and BC-R (Table 1), based on the *LvBCCIP* gene sequence, with Primer Premier v6.2 (<http://www.premierbiosoft.com>) [19]. After PCR amplification of the *LvBCCIP* gene sequence, the recombinant bait vector pGBKT7-*LvBCCIP* was constructed using the In-Fusion HD Cloning Kit (Clontech, USA), following the manufacturer's instructions. Next, the vector pGBKT7-*LvBCCIP* was hybridized with the Y2H library to identify the cellular protein interacting with *LvBCCIP* as described in Section 2.1. Preliminary results indicated that *L. vannamei* calmodulin (*LvCaM*) interacted with *LvBCCIP*.

Table 1

Primers used in this study. The primers 18s-F and 18s-R have been previously published [26]; all other primers were designed in this study using Primer Premier v6.2 (<http://www.premierbiosoft.com>). Underlining indicates restriction sites for cloning.

Name	Sequence (5'–3')
Primers for plasmid construction	
IN-F	GAGGACCTGCATATGATGTGCGCCGATTCAACAAGAGCA
IN-R	GGCCGAATTC <u>CCGGG</u> TGATTAGTATGCATAATAACA
BC-F	CATGGAGGCCGAATTCATGCTGCGCCGATGAAGAA
BC-R	GCAGGTCGACGGAT <u>CTC</u> CAATATACAGCATCTTTCATT
GST-CP-F	CGCGGATCCATGTGCGCCGATTCAACAAGAG
GST-CP-R	CCGCTCGAGCGTTAGTTAGTATGCATAATAACA
GST-CaM-F	CGCGGATCCATGGCTGATCAACTGACTGAAGAAC
GST-CaM-R	CCGCTCGAGCGGTCACTTCGAGGTCATCATC
V5- <i>LvBCCIP</i> -F	CGCGGATCCATGTCTGCGCCGATGAAGAAACC
V5- <i>LvBCCIP</i> -R	CCGCTCGAGCGATATACAGCATCTTTCATTTC
Primers for real-time quantitative PCR	
18s-F	GCCTGAGAAACGGCTACACATC
18s-R	GTAGTAGCGACGGGCGGTGTGT
<i>LvBCCIP</i> -F	ATGAAGGAATGGGTAAACGGTG
<i>LvBCCIP</i> -R	GCTGTCCTAAGACCTGCTATGC
PstDNV-F	CATGGAGGCCGAATTCATGTTATATCTCTATGGTCTAAAGAGC
PstDNV-R	GCAGGTCGACGGATCCITATTTAAGTTCGCTCCATTGGTCC
Primers for RNA interference	
T7- <i>LvBCCIP</i> -F	GGATCCTAATACGACTCACTATAGG TGCCAGCGATTCAACAACC
T7- <i>LvBCCIP</i> -R	GGATCCTAATACGACTCACTATAGGATGAGCACTCGTCGGTAAGG
<i>LvBCCIP</i> -F1	TGCCAGCGATTCAACAACC
<i>LvBCCIP</i> -R1	ATGAGCACTCGTCGGTAAGG
T7-egfp-F	GGATCCTAATACGACTCACTATAGGTTGCCCATCCTGGTCGAGCT
T7-egfp-R	GGATCCTAATACGACTCACTATAGGTCACGCTGCCGCTCCTCGAT

2.3. Preliminary verification of protein–protein interactions

Positive yeast colonies (identified based on sequencing results) grown in sections 2.1 and 2.2 were selected and cultured at 30 °C in the dark for 24 h. Yeast plasmids were extracted and co-transfected with pGBKT7-CP or pGBKT7-LvBCCIP into yeast Y187 (Clontech, USA). Alternatively, yeast plasmids were extracted and co-transfected with pGBKT7-CaM or pGBKT7-LvBCCIP into yeast Y187 (Clontech, USA). After culture at 30 °C for 24 h in the dark, yeast suspensions were spread on different SD/-Ade/-His/-Leu/-Trp/X- α -Gal/Aba plates. Plates were incubated at 30 °C in the dark for 5 days. Blue colonies were considered positive clones.

2.4. Glutathione S-transferase (GST) pulldown verification

2.4.1. Construction and expression of the pIZ-V5-LvBCCIP plasmid

The primers V5-LvBCCIP-F and V5-LvBCCIP-R (Table 1) were designed based on the LvBCCIP ORF sequence using Primer Premier (V 6.2) (<http://www.premierbiosoft.com>) [19]. After PCR amplification, the amplicons were ligated to vector pIZ-V5 to construct the pIZ-V5-LvBCCIP plasmid. The pIZ-V5-LvBCCIP plasmid was transfected into High-Five cells (Invitrogen, USA) using Cellfectin II kits (Invitrogen, USA), following the manufacturer's instructions. High-Five cells were sampled before and after transfection. Sampled cells were fixed with 4% paraformaldehyde, stained with 4',6-diamidino-2-phenylindole, and then incubated with rhodamine-labeled goat anti-mouse antibody at 30 °C in the dark for 2 h. We then observed the expression plasmid in the High-Five cells under a fluorescence microscope (Olympus, Japan). After 48 h of transfection, the medium was aspirated and the cells were washed once in phosphate buffer saline (PBS) (containing 1% Triton X-100 and 100 \times protease inhibitor). Washed cells were resuspended in 1 mL of pre-cooled PBS. The cell suspension was transferred to a 1.5 mL centrifuge tube, and sonicated on ice at 300 W for 15 min. After sonication, the solution was centrifuged at 14,000 \times g at 4 °C for 10 min. The supernatant was collected for GST pull-down.

2.4.2. Construction of the GST-CP and GST-CaM expression plasmids

The primers GST-CP-F, GST-CP-R, GST-CaM-F, and GST-CaM-R were designed based on the PstDNV genome sequence (GenBank accession no. NC_002190.2) [18] and the LvCaM gene sequence (GenBank accession no. HQ832611.1; Table 1) [23]. The expression plasmids pGEX-6P-1-CP and pGEX-6P-1-LvCaM were constructed and separately transfected into *Escherichia coli* strain BL21. The plasmid pGEX-6p-1 was transfected into *E. coli* strain BL21 as a control. Single colonies were selected and inoculated into 5 mL of Luria-Bertani (LB) culture medium (containing 100 μ g/mL ampicillin). We then added Isopropyl β -D-1-thiogalactopyranoside (IPTG) (Solitaire, China) to the culture medium to a final concentration of 0.5 mM. The bacterial solution was then cultured at 37 °C with shaking at 200 \times g until the optical density at 600 nm (OD₆₀₀) was 0.6. The culture was then induced for an additional 24 h at 16 °C with shaking at 200 \times g. After induction, cells were collected by centrifugation at 4 °C and 5000 \times g for 5 min, then resuspended in 5 mL PBS (containing 1% Triton X-100 and 100 \times protease inhibitor). The suspension was then sonicated on ice at 300 W for 30 min. The sonicated cells were centrifuged at 4 °C and 14,000 \times g for 10 min, and the supernatant was collected. We then detected the protein expression of GST-CP and GST-CaM in the supernatant using sodium dodecyl sulfate polyacrylamide gel electrophoresis (SDS-PAGE) analysis with Coomassie blue staining [24].

2.4.3. GST-pull down and western blot analysis

Aliquots of the supernatant prepared in Section 2.4.1 (containing the protein expressed by the pIZ-V5-LvBCCIP plasmid) were added three different glutathione agarose resins, bound to GST, GST-CP, or GST-CaM. The mixtures were incubated overnight at 4 °C with gentle shaking, and then centrifuged at 2000 \times g for 3 min. The supernatants

were removed. Each precipitate was rinsed five times with 1 mL of pre-cooled PBS, and centrifuged at 2000 \times g for 1 min. For each tube, the PBS was aspirated as much as possible, and then 50 μ L of 2 \times SDS loading buffer was added. Each mixture was placed in a boiling water bath for 10 min, and centrifuged at 12,000 \times g for 1 min. The supernatants were separated using SDS-PAGE [24], and the separated proteins were transferred to PVDF membranes (Amersham Biosciences, Sweden). The PVDF membranes were placed in blocking solution (5% w/v skim milk powder dissolved in 1 \times TBST, 20 mM Tris-HCl, 150 mM NaCl, and 0.1% Tween 20; pH 7.6) with the anti-V5-HRP antibody (diluted 1:5000 in the blocking solution; Life Technology, USA) at room temperature for 3 h. After incubation, each PVDF membrane was washed three times with TBST (10 min per wash), and then incubated with ECL chemiluminescence reagent [25] for 2 min at 30 °C. Membranes were then exposed using X-ray film.

2.5. Expression of LvBCCIP in *L. vannamei* after PstDNV challenge

Specific pathogen free *L. vannamei* were acclimated to the aquarium equipment for two days before the challenge. Shrimp were randomly divided into experimental and control groups (n = 36 per group). Each experimental shrimp was injected with 100 μ L of PstDNV solution ($\sim 10^6$ PstDNV copies/ μ L of solution), and each control shrimp was injected with 100 μ L PBS. At 0, 2, 4, 6, 8, 12, 24, 36, 48, 60, 72, and 84 h after injection, the hepatopancreas of three shrimp per group were collected for RNA extraction.

Total RNA was extracted from the hepatopancreas using TRIzol Reagent (Invitrogen, USA). qRT-PCR was performed with SYBR Premix Ex Taq™ II kits (TaKaRa, Japan), following the manufacturer's instructions. The qRT-PCR cycling program was as follows: preheating at 95 °C for 30 s; then 40 cycles of 95 °C for 5 s and 60 °C for 30 s. We used 18S RNA as the internal reference gene; 18S RNA was amplified using the primers 18s-F and 18s-R [26] (Table 1). The primers PstDNV-F and PstDNV-R for detection of viral titer were listed in Table 1. LvBCCIP was amplified using the primers LvBCCIP-F and LvBCCIP-R (Table 1), which were designed based on the LvBCCIP gene sequence using Primer Premier v 6.2 (<http://www.premierbiosoft.com>) [19]. Three parallel qRT-PCRs were performed for both the experimental and the control groups. The relative mRNA expression levels of LvBCCIP were calculated using the $2^{-\Delta\Delta CT}$ method [27], and significant differences in expression between the experimental and control groups were identified using Student's *t*-test. We considered *P* < 0.01 statistically significant.

2.6. Synthesis of dsRNA

dsRNAs were used to silence LvBCCIP gene expression. First, the enhanced green fluorescent protein gene (egfp) was synthesized using the T7 RiboMAX Express RNAi System (Promega, USA), following the manufacturer's instructions. The primers T7-LvBCCIP-F, T7-LvBCCIP-R, LvBCCIP-F1, and LvBCCIP-R1 (Table 1) were used to synthesize dsRNA-LvBCCIP. The primers T7-egfp-F, T7-egfp-R, egfp-F and egfp-R (Table 1) were used to synthesize dsRNA-egfp. The reaction contained 10 μ L RiboMAX™ express T7 2 \times Buffer, 1 μ g template DNA, 2 μ L enzyme mix, and nuclease-free water to make 20 μ L. The reaction volume was incubated at 37 °C for 3 h. The sense and antisense RNA strands were mixed in equal volumes and annealed at 70 °C for 10 min to form dsRNA.

2.7. Effects of LvBCCIP gene silencing on PstDNV proliferation

Specific pathogen-free (SPF) *L. vannamei* were randomly divided into three replicate control groups and three replicate treatment groups (n = 20 per group). Each shrimp in each treatment group was injected at the second abdominal segment with 20 μ g of dsRNA-LvBCCIP, while each shrimp in each control group was injected at the second abdominal segment with 20 μ g of dsRNA-egfp. Each shrimp was identically re-

injected after 24 h. At 0 h, 24 h, 36 h, 48 h, 60 h and 72 h after the first dsRNA injection, hemocyte samples were collected from three randomly-selected shrimp per group for RNA extraction. We then determined the efficacy of the dsRNA injection using qRT-PCR. The qRT-PCR cycling program was as follows: preheating at 95 °C for 30 s; then 40 cycles of 95 °C for 5 s and 60 °C for 30 s.

At 72 h after the first dsRNA injection, each shrimp was injected with 100 µL of the PstDENV solution ($\sim 10^6$ PstDENV copies/µL of solution). At 12 h, 24 h, 36 h, 48 h, 60 h, and 72 h after the PstDENV injection, three shrimp were selected from each replicate. We quantified the viral load of each shrimp using qRT-PCR. First, total genomic DNA was extracted from each shrimp using Marine Animal Genomic DNA Extraction kits (Tiangen, China), following the manufacturer's instructions. Next, genomic DNA was used as a template for qRT-PCR. We tested whether there was a significant difference in the viral load of the treatment group as compared to the control group using Student's *t*-test.

2.8. Effect of LvBCCIP gene silencing on shrimp growth

Specific pathogen-free *L. vannamei* were randomly divided into three replicate control groups and three replicate treatment groups ($n = 36$ per group). Each shrimp in each treatment group was injected with 20 µg dsRNA-LvBCCIP (diluted in 100 µL PBS), while each shrimp in each control group was injected with 20 µg dsRNA-egfp (diluted in 100 µL PBS). Each shrimp was identically re-injected after 24 h. Shrimp were then fed normally for 40 days, with a third identical dsRNA injection after the first 20 days. After 40 days, the body weight of each shrimp was measured. We tested whether there was a significant difference in body weight in the treatment group versus the control group using Student's *t*-test.

3. Results

3.1. Identification of the *L. vannamei* protein that interacts with PstDENV-CP

The titer of the cDNA Y2H library that we constructed from the muscle tissues of *L. vannamei* was more than 2.0×10^6 colony forming units (cfu)/ml, and the cell density was 1.7×10^8 cells/ml. We detected neither self-activation nor toxicity when the bait vector pGBKT7-CP was

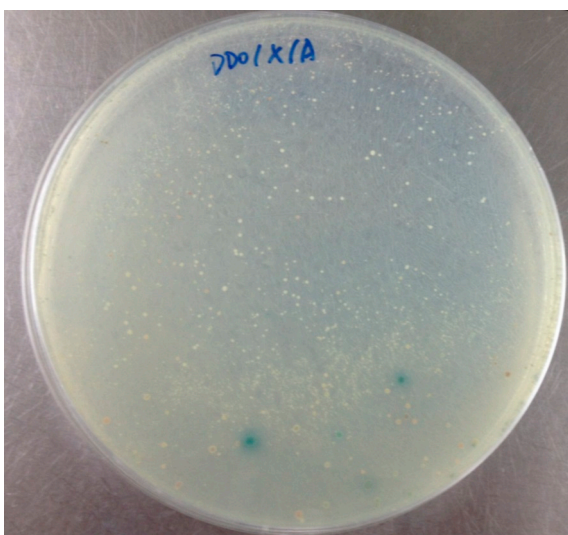


Fig. 1. Screening of the *Litopenaeus vannamei* cDNA library with the *Penaeus stylirostris* densovirus (PstDENV)-capsid protein, showing positive (blue) and negative (white) clones on SD/-Leu-Trp-His-Ade/X-α-Gal/Aba agar plates. (For interpretation of the references to colour in this figure legend, the reader is referred to the Web version of this article.)

introduced into yeast. After the introduced yeast was hybridized with the Y2H library, we selected 19 positive (blue) clones from those grown on SD/-Ade/-His/-Leu/-Trp/X-α-Gal/Aba plates (Fig. 1). All the sequences of the 19 positive clones were identical and were highly homologous to previously published BRCA2 and CDKN1A(p21)-interacting protein (BCCIP) gene sequences from other species, including mediterranean fruit fly (*Ceratitis capitata*) (accession no. JAC02094.1), Atlantic salmon (*Salmo salar*) (accession no. AC167438.1), colesseed sawfly (*Athalia rosae*) (accession no. XP_012255522.1), pharaoh ant (*Monomorium pharaonis*) (accession no. XP_012538062.1), common carp (*Cyprinus carpio*) (accession no. XP_018948384.1), Chinese hamster (*Cricetulus griseus*) (accession no. RLQ70359.1), tropical clawed frog (*Xenopus tropicalis*) (accession no. NP_001004968.1), salmon louse (*Lepeophtheirus salmonis*) (accession no. ADD24052.1), human (*Homo sapiens*) (accession no. AAL55438.1), climbing perch (*Anabas testudineus*) (accession no. XP_026206301.1), emu (*Dromaius novaehollandiae*) (accession no. XP_025971656.1), Nile tilapia (*Oreochromis niloticus*) (accession no. XP_003441823.1), Burmese python (*Python bivittatus*) (accession no. XP_007434157.1), rock pigeon (*Columba livia*) (accession no. PKK28042.1) and eastern oyster (*Crassostrea virginica*) (accession no. XP_022289211.1). We thus named the *L. vannamei* gene LvBCCIP. The LvBCCIP gene sequence was submitted to GenBank (accession no. KP247565). The LvBCCIP gene was 1027 base pairs (bp) long, and contained an 882 bp open reading frame (ORF), encoding 293 amino acids (aa) with a calculated molecular weight of 33.164 kDa and an isoelectric point of 4.336. Domain analysis of the LvBCCIP protein sequence revealed that LvBCCIP had a BCCIP domain characteristic of the BCCIP family. BLAST searches against GenBank showed that the BCCIP domain of LvBCCIP was highly conserved among species. Our NJ phylogenetic tree indicated that LvBCCIP formed a clade with the BCCIP proteins of other arthropods, distinct from the BCCIP proteins of vertebrates (Fig. 2).

3.2. Identification of the *L. vannamei* protein that interacts with LvBCCIP

To identify proteins interacting with LvBCCIP, we constructed the bait vector pGBKT7-BCCIP. We detected neither self-activation nor toxicity when the bait vector pGBKT7-BCCIP was introduced into yeast. After the introduced yeast was hybridized with the Y2H library, we selected 13 positive (blue) clones from those grown on SD/-4/X-α-Gal/Aba plates. Sequencing showed that their sequences were identical. BLAST searches against GenBank showed that the sequences of the 13 positive clones were highly homologous to the *L. vannamei* calmodulin (LvCaM) gene sequence. Thus, our preliminary results indicated that LvBCCIP interacted with LvCaM.

3.3. Preliminary verification of protein-protein interactions

Positive (blue) yeast colonies co-transformed with pGBKT7-CP and pGADT7-BCCIP grew on SD/-Ade/-His/-Leu/-Trp/X-α-Gal/Aba plates (Fig. 3A), as did positive (blue) yeast colonies co-transformed with pGBKT7-BCCIP and pGADT7-CaM (Fig. 3B). This preliminarily verified the interaction between PstDENV-CP and LvBCCIP, and between LvBCCIP and LvCaM.

3.4. GST-pulldown verification

To verify the PstDENV-CP/LvBCCIP and LvBCCIP/LvCaM interactions, we first constructed the expression plasmid pIZ-V5-LvBCCIP. After transfection, fluorescence microscopy showed that pIZ-V5-LvBCCIP was expressed in High-Five cells, suggesting that plasmid construction had been successful (Fig. 4). Our SDS-PAGE results indicated that the expression plasmids pGEX-6p-CP and pGEX-6p-LvCaM had been successfully constructed, and that the GST, GST-CP, and GST-CaM proteins were expressed in *E. coli* (Fig. 5). Our western blot results indicated that LvBCCIP was pulled down by both GST-CP (Fig. 6A) and

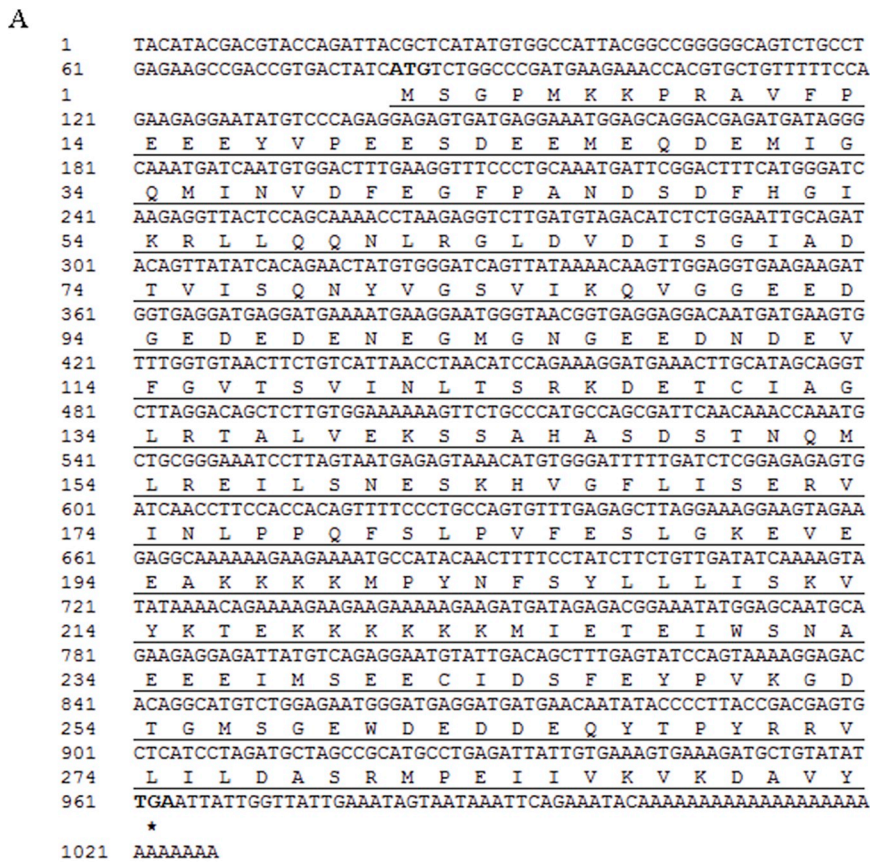
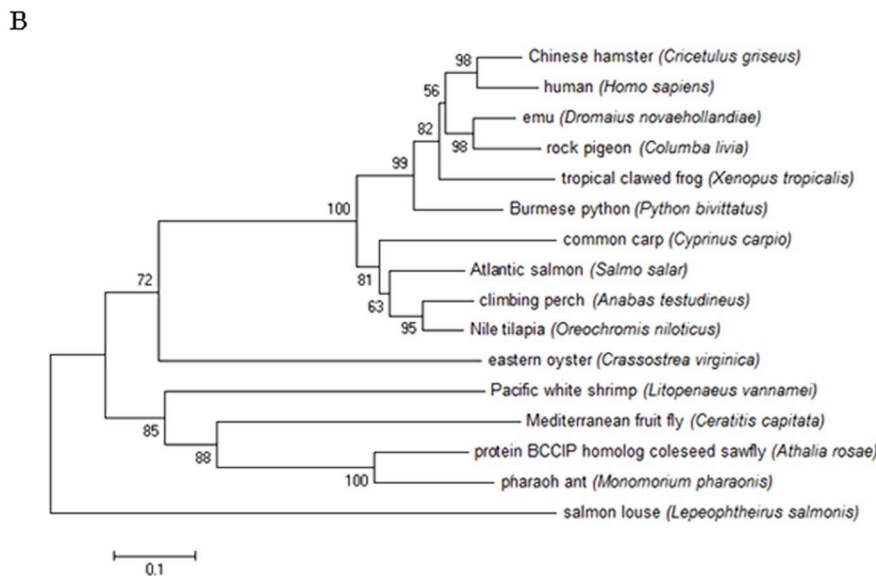


Fig. 2. Sequence analysis of *Litopenaeus vannamei* BCCIP. (A) Nucleotide and deduced amino acid sequences of *Litopenaeus vannamei* BCCIP. (B) Neighbor-joining phylogeny of the BCCIP proteins of *Litopenaeus vannamei* and fifteen other species, downloaded from GenBank and the accession numbers are as follows: *Ceratitis capitata* (JAC02094.1), *Salmo salar* (ACI67438.1), *Athalia rosae* (XP_012255522.1), *Monomorium pharaonis* (XP_012538062.1), *Cyprinus carpio* (XP_018948384.1), *Cricetulus griseus* (RLQ70359.1), *Xenopus tropicalis* (NP_001004968.1), *Lepeophtheirus salmonis* (ADD24052.1), *Homo sapiens* (AAL55438.1), *Anabas testudineus* (XP_026206301.1), *Dromaius novaehollandiae* (XP_025971656.1), *Oreochromis niloticus* (XP_003441823.1), *Python bivittatus* (XP_007434157.1), *Columba livia* (PKK28042.1), *Crassostrea virginica* (XP_022289211.1). The numbers at the branches show the percent bootstrap majority consensus values after 1,000 replicates.



GST-CaM (Fig. 6B). These results again suggested that PstDNV-CP and LvBCCIP interacted, as did LvBCCIP and LvCaM.

3.5. Expression of LvBCCIP in *L. vannamei* after PstDNV infection

Our qRT-PCR results showed that *LvBCCIP* gene expression levels were significantly higher than those of the uninfected control 36–72 h after PstDNV infection ($P < 0.05$), peaking at 48 h and returning to

basal levels at 84 h (Fig. 7). In contrast, *LvBCCIP* gene expression levels in the uninfected control remained stable throughout the observation period (0–84 h; Fig. 7).

3.6. In vivo interference with LvBCCIP gene expression

We next tested whether the injection of dsRNA-LvBCCIP would affect *LvBCCIP* gene expression in *L. vannamei*. Our qRT-PCR results

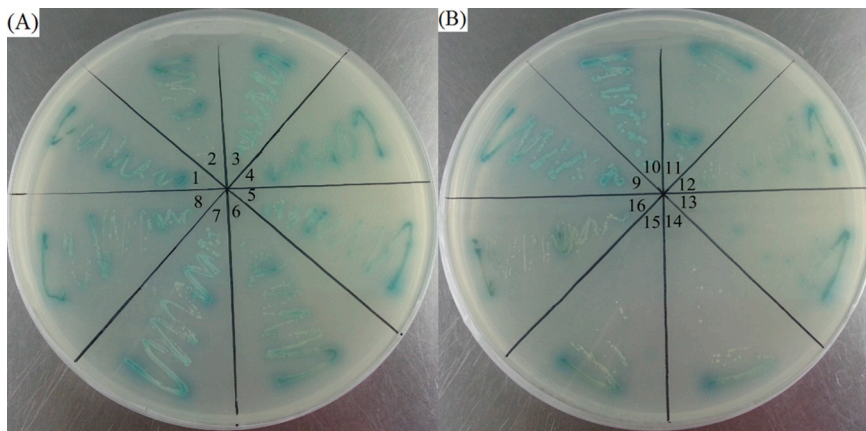


Fig. 3. Yeast two-hybrid (Y2H) verifications of the interactions between (A) the *Penaeus stylirostris* densovirus (PstDNV)-capsid protein and *Litopenaeus vannamei* BCCIP, and (B) *Litopenaeus vannamei* BCCIP and *Litopenaeus vannamei* calmodulin (CaM). Co-transfected yeast was spread on SD/-Ade/-His/-Leu/-Trp/X- α -Gal/Aba plates; blue colonies indicate a positive result. (For interpretation of the references to colour in this figure legend, the reader is referred to the Web version of this article.)

indicated that LvBCCIP gene expression was significantly down-regulated in the shrimp injected with dsRNA-LvBCCIP, as compared to those injected with dsRNA-egfp ($p < 0.01$; Fig. 8). This indicated that the injection of dsRNA-LvBCCIP effectively interfered with LvBCCIP gene expression.

3.7. Effects of LvBCCIP gene silencing on PstDNV proliferation

After injection with either dsRNA-LvBCCIP or dsRNA-egfp, shrimp were challenged with PstDNV. Our qRT-PCR results indicated that shrimp injected with dsRNA-LvBCCIP tended to have fewer copies of PstDNV 36–72 h after PstDNV injection, as compared to shrimp injected with dsRNA-egfp (Fig. 9). At 72 h after PstDNV injection, shrimp injected with dsRNA-LvBCCIP had significantly fewer copies of PstDNV than did shrimp injected with dsRNA-egfp ($p < 0.01$; Fig. 9). This suggested that the inhibition of LvBCCIP gene expression reduced PstDNV proliferation.

3.8. Effects of LvBCCIP gene silencing on the growth of *L. vannamei*

After injection with either dsRNA-LvBCCIP or dsRNA-egfp, shrimp were allowed to feed normally. After 40 days, the average body weight of shrimp injected with dsRNA-LvBCCIP was significantly lower than that of the shrimp injected with dsRNA-egfp ($p < 0.01$; Fig. 10). Thus, shrimp growth rate was significantly reduced after the inhibition of LvBCCIP gene expression.

4. Discussion

PstDNV is one of the most important viral pathogens affecting shrimp [5]. PstDNV infections in *L. vannamei*, although not lethal, cause RDS, which leads to slow growth and reduces economic value [10]. Therefore, the identification of interactions between PstDNV and host proteins increases our understanding, not only of RDS pathogenesis, but also of the regulatory proteins involved in shrimp growth.

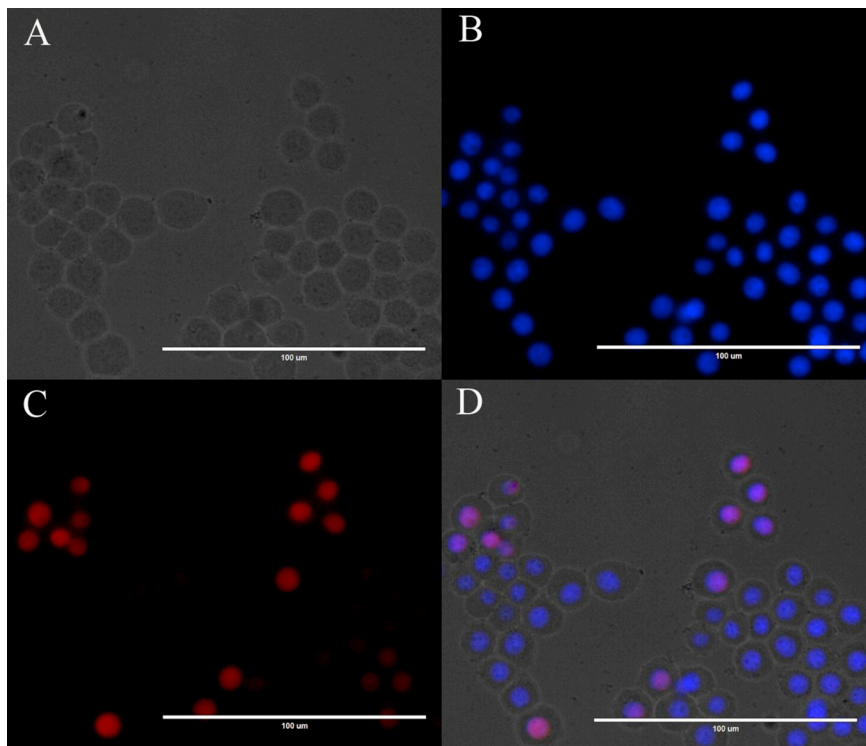


Fig. 4. Expression of the plasmid pIZ-V5-LvBCCIP in High-Five cells, as observed under a fluorescence microscope. (A) Unstained High-Five cells. Scale bar = 100 μ m. (B) High-Five cells stained with 4',6-diamidino-2-phenylindole; blue indicates the nucleus. Scale bar = 100 μ m. (C) High-Five cells treated with rhodamine-labeled goat anti-mouse antibody; red indicates LvBCCIP. Scale bar = 100 μ m. (D) Merge of (A), (B), and (C). Scale bar = 100 μ m. (For interpretation of the references to colour in this figure legend, the reader is referred to the Web version of this article.)

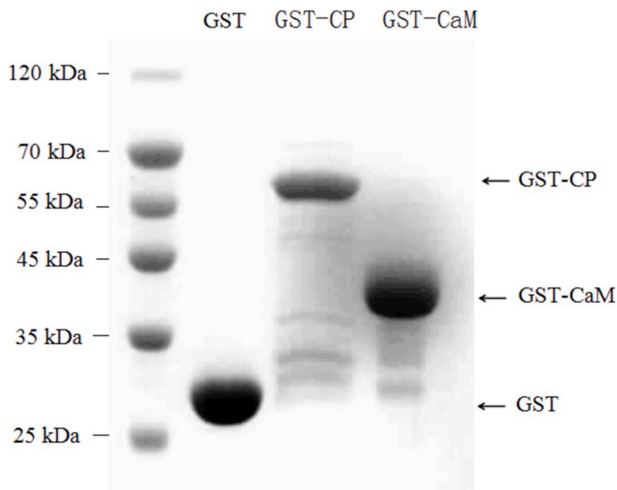


Fig. 5. Expression of GST, GST-CP, and GST-CaM plasmids in *Escherichia coli*, as detected by dodecyl sulfate polyacrylamide gel electrophoresis (SDS-PAGE) and Coomassie blue staining. The expected molecular weights of GST, GST-CP, and GST-CaM were 26.0 kDa, 63.4 kDa and 42.5 kDa, respectively.

As PstDNV encodes only three proteins, this virus is good model for studies of the interactions between viral and host proteins. However, the interactions between PstDNV proteins and host proteins have been little investigated. It has been reported that the protein encoded by PstDNV ORF2 interacts with actin in the shrimp *Marsupenaeus japonicus* [28], and that the PstDNV capsid protein interacts with troponin I in *L. vannamei* [29]. Here, our results indicated that PstDNV-CP interacted with LvBCCIP.

To the best of our knowledge, this is the first report of the cloning of a *BCCIP* gene in shrimp. *BCCIP*, originally identified as a BRCA2 and Cip1/p21 interacting protein, contains a sequence similar to the calcium-binding protein, calmodulin [30]. Thus, *BCCIP* is potentially a calcium-binding protein. The *BCCIP* gene is indispensable for cell survival and genetic stability, playing important roles in cell cycle regulation, the homologous recombination repair of DNA damage, and the maintenance of genomic stability [31]. Studies have shown that insufficient *BCCIP* inhibits ribosome function and S7 promoter function, restricting cell proliferation, and thereby affecting cell growth and tumor development [32,33]. However, most of the available studies of *BCCIP* function have been performed in human cells. Although *BCCIP* is highly conserved among vertebrates and invertebrates, the function of

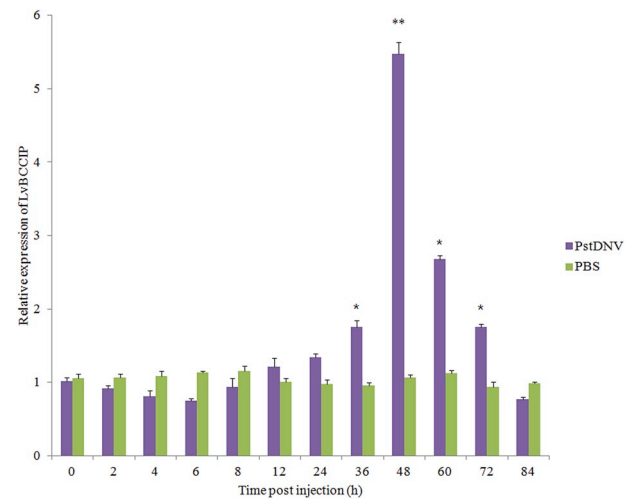


Fig. 7. *LvBCCIP* gene expression (relative to 18sRNA) in the hemocytes of *Litopenaeus vannamei* after challenge with *Penaeus stylirostris* densovirus (PstDNV; orange bars) or PBS (control; green bars). Asterisks above bars indicate a significant difference in relative gene expression as compared the control. *, $P < 0.05$; **, $P < 0.01$. The error bars show the standard deviation of three biological replicates. (For interpretation of the references to colour in this figure legend, the reader is referred to the Web version of this article.)

BCCIP in invertebrates has not been reported. Thus, the role of *BCCIP* in shrimp immunity remains unclear.

Our results also indicated that the LvCaM protein interacted with LvBCCIP. CaM, the primary intracellular and intramembranous calcium (Ca^{2+}) receptor, detects free Ca^{2+} and converts changes in Ca^{2+} concentration into metabolic states [34]. The CaM gene has been cloned in several shrimp species, including *Procambarus clarkia* [35], *Penaeus monodon* [36], *Crangon crangon* [37] and *L. vannamei* [23]. As one of the most important intracellular second messengers, Ca^{2+} plays a key role in signal transduction [38]. Signal transduction regulates cellular processes by activating various signaling pathways, including cell division, secretion and differentiation, nerve conduction, DNA replication and repair, muscle contraction, circulating nucleotide metabolism, and glycogen metabolism [39]. CaM binds and regulates a variety of protein targets, including protein kinases, phosphatases, phosphatases, and cytoskeletal proteins; in this way, CaM affects many different cellular functions [40]. In animals, CaM or CaM-associated signaling pathways are involved in host defense against bacterial infections, suggesting that

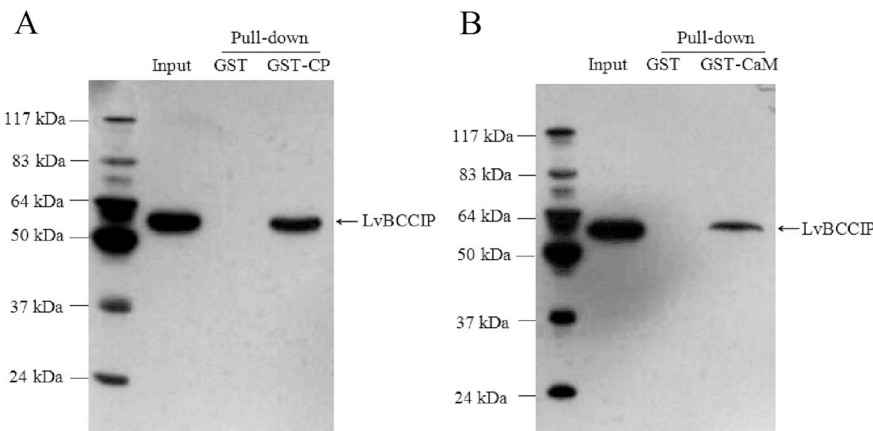


Fig. 6. Western blots showing the Glutathione S-transferase (GST) pull-down verifications of the interactions between (A) the *Penaeus stylirostris* densovirus (PstDNV)-capsid protein and *Litopenaeus vannamei* BCCIP, and (B) *Litopenaeus vannamei* BCCIP and *Litopenaeus vannamei* calmodulin (CaM). Input, expression proteins of GST, GST-CP, and GST-CaM plasmids.

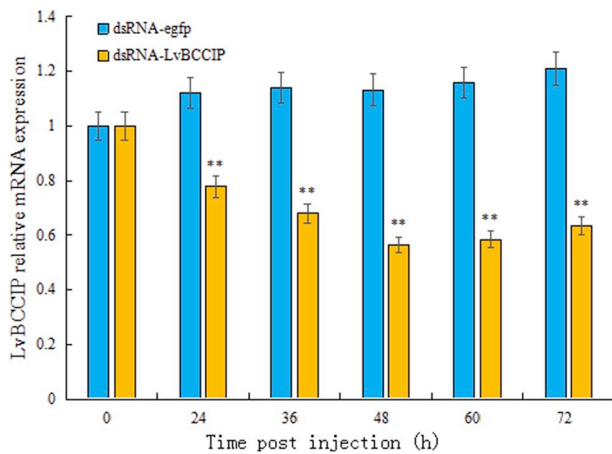


Fig. 8. *LvBCCIP* gene expression (relative to 18sRNA) after injection with double-stranded RNA (dsRNA) of *LvBCCIP* (orange bars) or dsRNA of the enhanced green fluorescent protein (*egfp*) gene (control; blue bars). Asterisks above bars indicate a significant difference in relative gene expression as compared the control. **, $P < 0.01$. The error bars show the standard deviation of three biological replicates. (For interpretation of the references to colour in this figure legend, the reader is referred to the Web version of this article.)

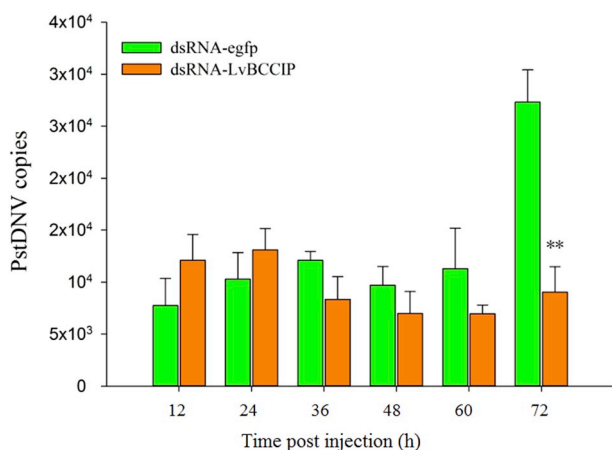


Fig. 9. Effects of *LvBCCIP* gene silencing on *Penaeus stylirostris* densovirus (PstDENV) proliferation. Orange bars represent shrimp in which *LvBCCIP* expression was inhibited using double-stranded RNA; green bars represent controls, in which *LvBCCIP* expression was unchanged. Asterisks above bars indicate a significant difference in relative gene expression as compared the control. **, $P < 0.01$. The error bars show the standard deviation of three biological replicates. (For interpretation of the references to colour in this figure legend, the reader is referred to the Web version of this article.)

CaM may play an important role in immunity [41]. In a recent study, CaM was identified as a potential regulator of growth of belonoid fishes [42].

Therefore, we speculated that *LvBCCIP* might affect the growth and immunity of *L. vannamei* by interacting with *LvCaM*. Indeed, our results showed that the inhibition of *LvBCCIP* gene expression significantly reduced shrimp body weight, indicating that *LvBCCIP* is an important regulator of body growth in *L. vannamei*. As PstDENV-CP interacted with *LvBCCIP*, this interaction might explain why PstDENV infection leads to RDS in shrimp. However, it remains unclear whether *LvBCCIP* interacts with additional proteins to affect shrimp growth; this question requires further study. In addition, when *LvBCCIP* gene expression in *L. vannamei* was inhibited, the proliferation of PstDENV was significantly reduced. This indicated that *LvBCCIP* plays an essential role in the proliferation of PstDENV. However, the mechanisms underlying this effect require further study.

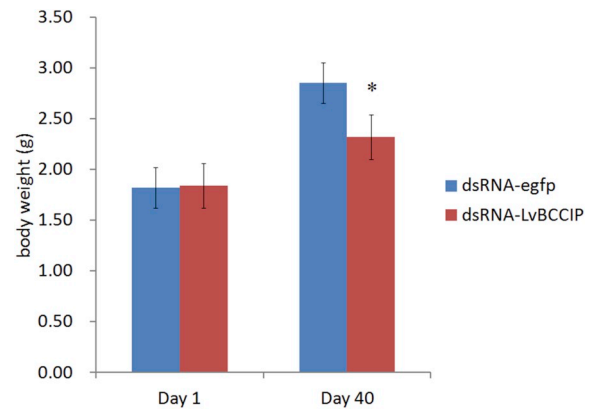


Fig. 10. Effects of *LvBCCIP* gene silencing on the growth of *Litopenaeus vannamei*. Red bars represent shrimp in which *LvBCCIP* expression was inhibited using double-stranded RNA; blue bars represent controls, in which *LvBCCIP* expression was unchanged. *, $P < 0.01$. The error bars show the standard deviation of three biological replicates. (For interpretation of the references to colour in this figure legend, the reader is referred to the Web version of this article.)

Acknowledgements

This study was supported by the Guangxi Natural Science Foundation (2018GXNSFAA294140), Scientific and Technological Innovation Major Base of Guangxi (AA17204088-1), Guangxi scientific research and technology development project (AB16380189, AB16380067), Scientific and Technological Innovation Major Base of Guangxi (AA17204080-1), the national modern agriculture industry technology system project (nycytxgxcxt-14-01), Modern Agroindustry Technology Research System (CARS-48), Eight Osmanthus scholars special funding (BGXZ-NMBDX-04).

References

- [1] I. Pérez Farfante, B.F. Kensley, Penaeoid and Sergestoid Shrimps and Prawns of the World: Keys and Diagnoses for the Families and Genera, Editions du Muséum, Paris, 1997.
- [2] S. Zeng, Z. Huang, D. Hou, J. Liu, S. Weng, J. He, Composition, diversity and function of intestinal microbiota in pacific white shrimp (*Litopenaeus vannamei*) at different culture stages, *PeerJ* 5 (2017) e3986.
- [3] C.H. Seibert, A.R. Pinto, Challenges in shrimp aquaculture due to viral diseases: distribution and biology of the five major penaeid viruses and interventions to avoid viral incidence and dispersion, *Braz. J. Microbiol.* 43 (2012) 857–864 [publication of the Brazilian Society for Microbiology].
- [4] P. Sithigorngul, W. Hajimasaleh, S. Longyant, P. Sridulyakul, S. Rukpratanporn, P. Chaivisuthangkura, Simple immunoblot and immunohistochemical detection of *Penaeus stylirostris* densovirus using monoclonal antibodies to viral capsid protein expressed heterologously, *J. Virol Methods* 162 (2009) 126–132.
- [5] F. Mendoza-Cano, T. Enriquez-Espinoza, T. Encinas-García, A. Sanchez-Paz, Prevalence of the infectious hypodermal and hematopoietic necrosis virus in shrimp (*Penaeus vannamei*) broodstock in northwestern Mexico, *Prev. Vet. Med.* 117 (2014) 301–304.
- [6] J.R. Bonami, B. Trumper, J. Mari, M. Brehelin, D.V. Lightner, Purification and characterization of the infectious hypodermal and hematopoietic necrosis virus of penaeid shrimps, *J. Gen. Virol.* 71 (Pt 11) (1990) 2657–2664.
- [7] Y.A. Lu, E.C. Nadala Jr., J.A. Brock, P.C. Loh, A new virus isolate from infectious hypodermal and hematopoietic necrosis virus (IHNV)-infected penaeid shrimps, *J. Virol Methods* 31 (1991) 189–195.
- [8] J.H. Kim, H.K. Kim, V.G. Nguyen, B.K. Park, C.H. Choresca, S.P. Shin, J.E. Han, J.W. Jun, S.C. Park, Genomic sequence of infectious hypodermal and hematopoietic necrosis virus (IHNV) KLV-2010-01 originating from the first Korean outbreak in cultured *Litopenaeus vannamei*, *Arch. Virol.* 157 (2012) 369–373.
- [9] Y. Lu, P.C. Loh, J.A. Brock, Isolation, purification and characterization of infectious hypodermal and hematopoietic necrosis virus (IHNV) from penaeidshrimp, *J. Virol Methods* 26 (1989) 339–343.
- [10] K. Chayaburakul, D.V. Lightner, S. Sriurairattana, K.T. Nelson, B. Withyachumarnkul, Different responses to infectious hypodermal and hematopoietic necrosis virus (IHNV) in *Penaeus monodon* and *P. vannamei*, *Dis. Aquat. Org.* 67 (2005) 191–200.
- [11] J.A. Cowlley, M. Rao, G.J. Coman, Real-time PCR tests to specifically detect IHNV lineages and an IHNV EVE integrated in the genome of *Penaeus monodon*, *Dis. Aquat. Org.* 129 (2018) 145–158.

- [12] C.L. Browdy, J.D. Holloway, C.O. King, A.D. Stokes, J.S. Hopkins, P.A. Sandifer, IHNN virus and intensive culture of *Penaeus vannamei*: effects of stocking density and water exchange rates, *J. Crustac Biol.* 13 (1993) 87–94.
- [13] C.A. Horvath, G.A. Boulet, V.M. Renoux, P.O. Delvenne, J.P. Bogers, Mechanisms of cell entry by human papillomaviruses: an overview, *Virology* 7 (2010) 11.
- [14] A. Luque, D. Reguera, The structure of elongated viral capsids, *Biophys. J.* 98 (2010) 2993–3003.
- [15] H. van Steeg, M. Kasperaitis, H.O. Voorma, R. Benne, Infection of neuroblastoma cells by Semliki Forest virus. The interference of viral capsid protein with the binding of host messenger RNAs into initiation complexes is the cause of the shut-off of host protein synthesis, *Eur. J. Biochem.* 138 (1984) 473–478.
- [16] S.Y. Lu, Y.P. Qi, G.Q. Ge, Interaction of *Heliothis armigera* nuclear polyhedrosis viral capsid protein with its host actin, *J. Biochem. Mol. Biol.* 35 (2002) 562–567.
- [17] L. Guarente, Strategies for the identification of interacting proteins, *Proc. Natl. Acad. Sci. U. S. A* 90 (1993) 1639–1641.
- [18] L.M. Numan, B.T. Poulos, D.V. Lightner, Use of polymerase chain reaction for the detection of infectious hypodermal and hematopoietic necrosis virus in penaeid shrimp, *Mar. Biotechnol.* 2 (2000) 319–328.
- [19] V.K. Singh, A.K. Mangalam, S. Dwivedi, S. Naik, Primer premier: program for design of degenerate primers from a protein sequence, *Biotechniques* 24 (1998) 318–319.
- [20] S.F. Altschul, W. Gish, W. Miller, E.W. Myers, D.J. Lipman, Basic local alignment search tool, *J. Mol. Biol.* 215 (1990) 403–410.
- [21] E.L. Sonnhammer, S.R. Eddy, R. Durbin, Pfam: a comprehensive database of protein domain families based on seed alignments, *Proteins* 28 (1997) 405–420.
- [22] S. Kumar, K. Tamura, M. Nei, MEGA: molecular evolutionary genetics analysis software for microcomputers, computer applications in the biosciences, *CABIOS* 10 (1994) 189–191.
- [23] P.F. Ji, C.L. Yao, Z.Y. Wang, Two types of calmodulin play different roles in Pacific white shrimp (*Litopenaeus vannamei*) defenses against *Vibrio parahaemolyticus* and WSSV infection, *Fish Shellfish Immunol.* 31 (2011) 260–268.
- [24] S. Gallagher, J. Sasse, Protein analysis by SDS-PAGE and detection by Coomassie blue or silver staining, *Current protocols in pharmacology*, Appendix 3 (2001) 3B.
- [25] E. Manaresi, P. Pasini, G. Gallinella, G. Gentilomi, S. Venturoli, A. Roda, M. Zerbin, M. Musiani, Chemiluminescence Western blot assay for the detection of immunity against parvovirus B19 VP1 and VP2 linear epitopes using a videocamera based luminograph, *J. Virol Methods* 81 (1999) 91–99.
- [26] Q. Zhang, F. Li, X. Zhang, B. Dong, J. Zhang, Y. Xie, J. Xiang, cDNA cloning, characterization and expression analysis of the antioxidant enzyme gene, catalase, of Chinese shrimp *Fenneropenaeus chinensis*, *Fish Shellfish Immunol.* 24 (2008) 584–591.
- [27] K.J. Livak, T.D. Schmittgen, Analysis of relative gene expression data using real-time quantitative PCR and the 2(-Delta Delta C(T)) Method, *Methods* 25 (2001) 402–408.
- [28] G. Yang, X. Xiao, D. Yin, X. Zhang, The interaction between viral protein and host actin facilitates the virus infection to host, *Gene* 507 (2012) 139–145.
- [29] X. Chen, D. Zeng, W. Zhu, M. Peng, C. Yang, Q. Li, Q. Liu, Q. Yang, H. Wang, M. Li, Y. Lin, Y. Zhao, The *Penaeus stylirostris* densovirus capsid interacts with *Litopenaeus vannamei* troponin I, *Fish Shellfish Immunol.* 86 (2018) 101–106.
- [30] X. Meng, J. Liu, Z. Shen, Genomic structure of the human BCCIP gene and its expression in cancer, *Gene* 302 (2003) 139–146.
- [31] S.C. Huhn, J. Liu, C. Ye, H. Lu, X. Jiang, X. Feng, S. Ganesan, E. White, Z. Shen, Regulation of spindle integrity and mitotic fidelity by BCCIP, *Oncogene* 36 (2017) 4750–4766.
- [32] R. Droz-Rosario, H. Lu, J. Liu, N.A. Liu, S. Ganesan, B. Xia, B.G. Haffty, Z. Shen, Roles of BCCIP deficiency in mammary tumorigenesis, *Breast Cancer Res.* 19 (2017) 115.
- [33] Q. Ba, X. Li, C. Huang, J. Li, Y. Fu, P. Chen, J. Duan, M. Hao, Y. Zhang, C. Sun, H. Ying, H. Song, R. Zhang, Z. Shen, H. Wang, BCCIPbeta modulates the ribosomal and extraribosomal function of S7 through a direct interaction, *J. Mol. Cell Biol.* 9 (2017) 209–219.
- [34] C.B. Klee, T.C. Vanaman, Calmodulin, *Adv. Protein Chem.* 35 (1982) 213–321.
- [35] Y. Gao, C.M. Gillen, M.G. Wheatly, Cloning and characterization of a calmodulin gene (CaM) in crayfish *Procambarus clarkii* and expression during molting, *Comp. Biochem. Physiol. B Biochem. Mol. Biol.* 152 (2009) 216–225.
- [36] P. Sengprasert, P. Amparyup, A. Tassanakajorn, R. Wongpanya, Characterization and identification of calmodulin and calmodulin binding proteins in hemocyte of the black tiger shrimp (*Penaeus monodon*), *Dev. Comp. Immunol.* 50 (2015) 87–97.
- [37] R.H. Michael, R. Pipkorn, A. Willig, P.P. Jaros, Isolation and purification of calmodulin from the shrimp, *Crangon crangon*, *Life Sci.* 51 (1992) 1881–1889.
- [38] M. Nebel, B. Zhang, F. Odoardi, A. Flugel, B.V. Potter, A.H. Guse, Calcium signalling triggered by NAADP in T cells determines cell shape and motility during immune synapse formation, *Messenger (Los Angel)* 4 (2015) 104–111.
- [39] A.R. Means, J.R. Dedman, Calmodulin—an intracellular calcium receptor, *Nature* 285 (1980) 73–77.
- [40] S.W. Vetter, E. Leclerc, Novel aspects of calmodulin target recognition and activation, *Eur. J. Biochem.* 270 (2003) 404–414.
- [41] K.J. Wang, H.L. Ren, D.D. Xu, L. Cai, M. Yang, Identification of the up-regulated expression genes in hemocytes of variously colored abalone (*Haliotis diversicolor* Reeve, 1846) challenged with bacteria, *Dev. Comp. Immunol.* 32 (2008) 1326–1347.
- [42] H.M. Gunter, C. Koppermann, A. Meyer, Revisiting de Beer's textbook example of heterochrony and jaw elongation in fish: calmodulin expression reflects heterochronic growth, and underlies morphological innovation in the jaws of belonoid fishes, *EvoDevo* 5 (2014) 8.